# A COMPARATIVE STUDY ON TITANIUM-REINFORCED ALUMINIUM MATRIX COMPOSITES PRODUCED BY MELT INFILTRATION CASTING AND SQUEEZE INFILTRATION

**Ridvan Gecu and Ahmet Karaaslan**
Department of Metallurgical and Materials Engineering, Yildiz Technical University, Istanbul, Turkey

Copyright © 2018 American Foundry Society
https://doi.org/10.1007/s40962-018-0253-0

## Abstract

*The unresolved production problems including wettability and undesired intermetallic phase formation at the interface of aluminium matrix composites (AMCs) with ceramic reinforcements require a different approach to the subject. Titanium as a reinforcement is a strong candidate to overcome the current problems, without sacrificing beneficial features of conventional AMCs. This study aims to compare microstructural, mechanical and wear properties of bimetal composites manufactured by two different techniques: melt infiltration casting (MIC) and squeeze infiltration (SI). The temperature was set to 730 °C for both production methods. MIC was carried out in an open die with vacuum assistance, while SI was performed in a closed die in an atmospheric environment. Optical microscope, SEM, XRD, EDS, nanoindentation test device and ball-on-disc type tribometer with 3-mm-diameter $Al_2O_3$ ball were used for composite characterization. Al, Ti, Si and $TiAl_3$ phases were formed in composite structure for both techniques. Homogeneous and continuous $TiAl_3$ layer was obtained at Al/Ti interfaces. The volume fraction of $TiAl_3$ was 20 times higher in SI than that in MIC due to long interaction time between Al and Ti. The thickness and the hardness of $TiAl_3$ obtained were higher in SI. Abrasive and adhesive wear mechanisms were observed in worn surface examinations. The composite produced by SI showed slightly better performance against wear under the same test conditions. It was exposed to less plastic deformation and abrasive wear than composite produced by MIC. Although initial investment cost was higher, SI appeared to be more advantageous than MIC, considering the applicability in the industry.*

***Keywords:*** *melt infiltration casting, squeeze infiltration, bimetal composite production, interface characterization, wear*

## Introduction

Metal matrix composites (MMCs) have been widely used in automotive, aerospace, military and electronic industries owing to their high specific strength, high specific modulus, wear resistance and thermal stability.[1] The improvement in the mechanical properties of monolithic alloys is provided by micro- or nanoscale reinforcements.[2] The most attractive reinforcements in MMCs are ceramics, especially SiC particles owing to their high modulus and high fracture toughness, by comparison with the alternatives.[3] SiC particles have been mostly reinforced to aluminium alloys which show beneficial properties like facility of production, low density and high specific strength.[4] Still, unresolved problems of these particles including poor wettability,[5] decreasing toughness and ductility of matrix[6] and detrimental reaction phase formation[7] need a different approach to the issue. Metal reinforcements can be used in order to get rid of these negativities of the ceramics. Metal-reinforced MMCs offer competitive tribomechanical features without losing ductility and toughness of the matrix alloy.[8]

Al matrix composites (AMCs) with conventional ceramic reinforcements have been preferred to fabricate engine blocks, disc rotor brakes, cylinder heads and engine pistons in automotive industry.[9] In the production of these composites, which are preferred in such wide application fields, the cost of automobile components is as important as their lightness. From this standpoint, ceramic-reinforced AMCs seem disadvantageous in terms of economy because intrinsic lack of wetting and the undesired phase formation

at the interface cause difficulties during production. To overcome these problems, additional processes such as metal coating or hybridization are required. On the other hand, it is possible to manufacture metal-reinforced AMCs economically and environmentally friendly by selecting suitable methods and recyclable materials.[10]

Titanium is a strong candidate to replace ceramic reinforcements due to its low density, high modulus and high fatigue strength.[11] When Ti and Al alloys are combined, $TiAl_3$ phase is precipitated as a first product of the interfacial reaction. This phase enhances structural efficiency and thermal stability due to its low density ($\sim$ 3.3 g/cm$^3$), high melting temperature ($\sim$ 1400 °C), high hardness (500–610 HV) and good oxidation resistance.[12,13] $TiAl_3$ is a phase with the highest microhardness, the lowest density and the best oxidation resistance among all titanium aluminide compounds.[14] Although it shows low ductility at room temperature due to the low symmetry of its tetragonal DO22 structure, it has been proven that $TiAl_3$ phase prevents crack propagation by transferring the applied load from matrix to reinforcement by providing a coherent, clean and tight interface.[15] It should not be forgotten that the production temperature must be checked to beware of unwanted phase formations like $Al_2O_3$ or $TiO_2$.[16]

Conventional AMCs have been manufactured by various methods like powder metallurgy,[17] squeeze casting[18] and stir casting.[19] However, metal-reinforced AMCs cannot be manufactured by every method. Karthik et al.[20] stated that stir casting method is not suitable for bimetal composite production. Hassan and Gupta[21] offered a new technique called disintegrated melt deposition (DMD) instead of stir casting. Alongside the production methods mentioned, there are two other techniques to manufacture AMCs: (1) melt infiltration casting (MIC) and (2) squeeze infiltration (SI). These methods have huge potential to produce bimetal composites with very high volume fraction of reinforcement phase.[22] Unlike conventional AMCs, bimetal composites can be manufactured with very high volume fraction and consequently much improvement in wear resistance becomes possible. Both methods are based on the infiltration of molten Al alloy. Al melt is poured onto preform made by the shavings of reinforcements under vacuum atmosphere in MIC, while preform made by shavings of both matrix and reinforcement is heated above the melting temperature of Al and held in closed die in SI.

Although the production of preform-based AMCs has been investigated by several researchers,[23–25] metal usage in AMC manufacturing was not studied before. In this study, 75% Ti-reinforced A356 matrix bimetal composites were produced by MIC and SI methods at 730 °C. Microstructural, mechanical and wear properties of bimetal composites were investigated, and the effects of production method were compared.

## Experimental procedure

### Material selection

Bimetal composite structure is formed by the addition of commercially pure (Grade 2) Ti-to-Al matrix. A356 alloy was selected as matrix material because it has been widely used in the automobile industry due to its excellent pourability and fluidity features. However, this alloy exhibits poor resistance against sliding contact applications. The reason for Ti addition with very high volume is reducing the weakness of A356 matrix. Chemical compositions of A356 as a matrix and Ti as a reinforcement are listed in Table 1. The purity and the average size of Ti reinforcements were 99.4% and 150 μm, respectively. All composite components were supplied from recycled products for both production methods. Low cost and environmentally friendly production is the most important advantage of metal-reinforced AMCs against conventional AMCs.

### Composite production via melt infiltration casting (MIC)

Preform preparing, mould making and casting are the three main stages of the MIC process. In preform preparing step, strips of ribbon-shaped Ti shavings were gathered together under 330 MPa pressure. By means of mechanical compaction, 75% porous one-piece preform with the dimensions of 20 mm in diameter and 10 mm in height was attained.

In mould making step, 500 g investment powder and 200 g water were mixed for 3 min to prepare castable plaster slurry. Wax pattern was placed in stainless steel perforated flask and covered by the slurry under vibration. After solidification of the slurry, perforated flask was heated to 110 °C for wax pattern removal. Dewaxed mould was gradually heated up to 700 °C to ensure complete removal of residual carbon and water from the mould cavity.

The final step, casting, is illustrated in Figure 1. The plaster mould was taken from the furnace at 700 °C and settled in a vacuum chamber. Non-preheated preform made by Ti shavings was placed in the mould, and molten A356 alloy at 730 °C was poured onto preform. The casting temperature of A356 alloy and treatment temperature of the

***Table 1. Chemical Compositions of A356 Matrix and Ti Reinforcement (wt%)***

| Alloy | C | Si | Mn | O | Mg | Cu | Zn | Fe | Ti | Al |
|---|---|---|---|---|---|---|---|---|---|---|
| A356 | – | 7.0 | 0.1 | – | 0.35 | 0.2 | 0.1 | 0.2 | 0.2 | Bal. |
| Ti | 0.1 | – | – | 0.2 | – | – | – | 0.3 | Bal | – |

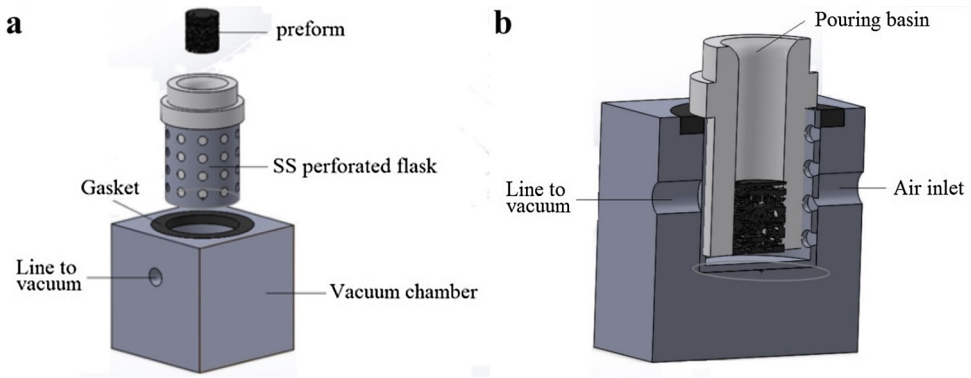


***Figure 1. Illustration of melt infiltration casting: (a) general view, (b) cross-sectional view.***

plaster mould were chosen close to each other to provide long liquid–solid interaction time. Al melt infiltrated the vacancies of the preform under $10^{-5}$ Pa vacuum pressure. After complete solidification of A356 alloy, perforated flask was taken out from the chamber and quenched. 75% of Ti-reinforced A356 matrix composite production via MIC was accomplished after quenching.

## Composite production via squeeze infiltration (SI)

SI technique, illustrated in Figure 2, was developed to eliminate the disadvantages of time-consuming MIC method. This technique does not require mould making step and vacuum environment for each composite production. It consists of two steps including preform preparing and infiltration. The mixture of A356 and Ti shavings were assembled under pressure to obtain porous monoblock preform. Specially designed closed die for infiltration process was fabricated by using H13 hot work tool steel. Preform was placed in a closed die and the die was placed in a furnace. The temperature was set at 730 °C. At this temperature, Al alloy was melted and diffused in preform vacancies and solid Ti. During melting of A356, cover die moved downwards and compressed the preform between base fitting and cover die. By means of 4.5 MPa pressure and 730 °C temperature, Al infiltration into Ti occurred. After holding at 730 °C for 1 h, the die was furnace-cooled. After cooling, composite sample was taken out and 75% Ti-reinforced A356 matrix composite production via SI was completed. Preforms used in both MIC and SI techniques are shown in Figure 3.

## Characterization

Bimetal composites were transversely cut by cutting device (Bulucut-1) for cross-sectional analysis. Cross sections of specimens were ground with SiC sandpapers and polished with 1 μm diamond paste. After metallographic preparation, microstructures were displayed via light optical microscope (Nikon Eclipse MA100) and scanning electron microscope (SEM, Hitachi SU3500 T2). X-ray diffraction (XRD, Philips PW 3710) analysis using CuKα radiation over $2\theta$ range of 10°–90° was performed to determine formed phases in composite structure. Energy-dispersive X-ray spectroscopy (EDS, Oxford XACT) was used to determine elemental composition of the reaction phases. The thickness of interfacial phases was measured via image

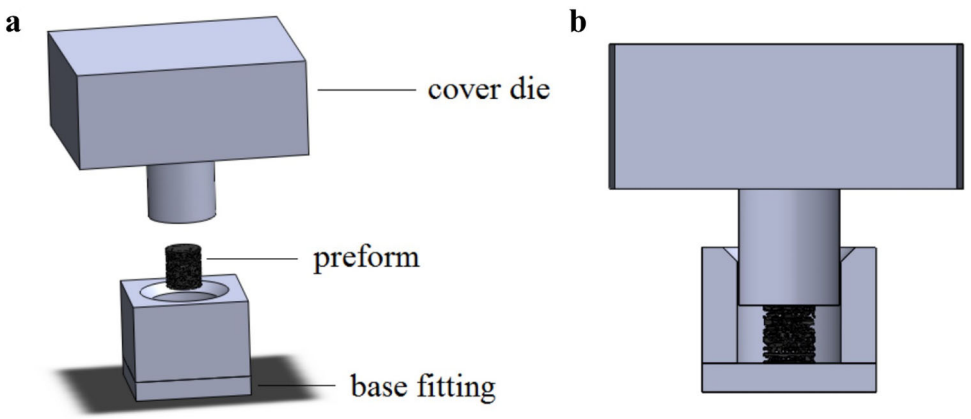


***Figure 2. Illustration of squeeze infiltration: (a) general view, (b) cross-sectional view.***

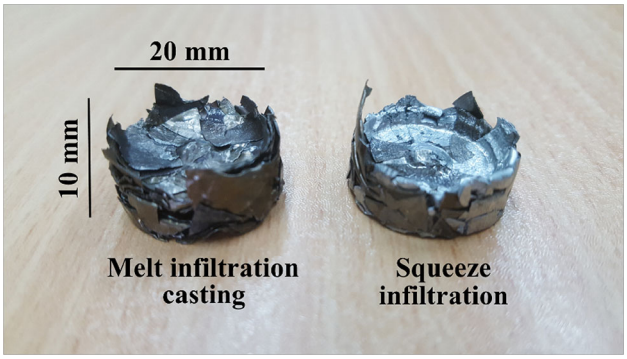


***Figure 3. Preforms used in melt infiltration casting and squeeze infiltration processes.***

analyser software (Zeiss), while their hardness was calculated by nanoindentation test device (CSM NHT, SN 06-177). 100 mN load in 120 steps with the interval of 1 s was applied to individual phases for 10 times with Berkovich indenter. After 10 s dwell time at 100 mN, the load was removed in 60 steps with the interval of 1 s. The average results of these measurements were given as a function of production method.

Ball-on-disc type wear tests were carried out by using 3-mm-diameter $Al_2O_3$ ball as a counter material. Table 2 gives the information about the condition of counter ball. It is aimed to determine severe wear behaviour of the composite structures by using $Al_2O_3$. The hardness of the ball is considerably higher than the components of the composite. 10 N load was applied to polished surfaces with $R_A$ = 0.45 µm. The rotating speed was 2 m/min and sliding distance was 100 m. Three wear tests were performed according to ASTM G99-17 for each sample, and the average volume losses and wear rates were measured by using following equations where V is volume loss, R is wear scar radius (2.5 mm), r is ball radius (1.5 mm), d is wear track width, $W_R$ is wear rate, L is sliding distance (100 m), and P is applied load (10 N).

$$V = 2\pi R\left[r^2 \sin^{-1}(d/2r) - (d/4)\left(4r^2 - d^2\right)^{1/2}\right] \quad \text{Eqn. 1}$$

$$W_R = \frac{V}{LP} \quad \text{Eqn. 2}$$

***Table 2. Specifications of $Al_2O_3$ Ball as a Counter Material***

| Speciality | Criteria | Speciality | Criteria |
|---|---|---|---|
| Purity (%) | 99.5 | Hardness (HV10) | 1410 |
| Size (mm) | Φ3 | Young's modulus (GPa) | 370 |
| Density (g/cm$^3$) | 3.86 | Compressive strength (MPa) | 2600 |
| Colour | White | Water absorption (%) | < 0.01 |

The test apparatus for wear tests is illustrated in Figure 4. When sliding tests were completed, the samples were examined by SEM for worn surface analysis. Worn surfaces were explained depending upon the production method comparatively.

## Results and Discussion

Figure 5 shows the XRD analysis results of Ti-reinforced A356 composites produced by both MIC and SI techniques. The reflexes of Al, Ti, Si and $TiAl_3$ were obtained in the diffractograms. A356 is a hypoeutectic Al alloy that consists of α-Al and eutectic (α-Al + Si) phases. Al and Si peaks were identified in XRD results because of the nature of A356 alloy. Only α-Ti peaks were obtained in Ti phase because the reinforcement phase did not exhibit any phase transformations at 730 °C. When A356 melt interacts with Ti, the first reaction product must be $TiAl_3$ according to Al–Ti phase diagram.[26] The interaction time between A356 and Ti was long enough to form $TiAl_3$ but not enough to form other Ti-rich titanium aluminide compounds such as $TiAl_2$ and TiAl. To beware of the problems that could occur because of the differences in crystal structures of possible titanium aluminide compounds, single-layer formation at the interface was preferred. As a result, only $TiAl_3$ reflexes were obtained in XRD analysis.

The micrographs of Ti-reinforced A356 matrix composites are given in Figure 6. All formed phases were marked in the images. α-Al and eutectic phases in A356 matrix can be clearly seen in Figure 6a. White α-Al grains were surrounded by light grey eutectic phases. Strong mechanical and metallurgical bonding occurred in both production methods. The strength of the interface bonding was achieved via vacuum assistance in MIC, while cover die pressure is the main reason for the bonding strength in SI. Homogeneous and continuous interface layer called $TiAl_3$ according to XRD results was formed at all interfaces. The first thing that stands out in Figure 6 was the differences in volume fraction of $TiAl_3$ layers. Almost all of Ti reinforcement was covered by $TiAl_3$ phase in SI method. It can be understood that the amount of Al diffusion into Ti was higher in SI than in MIC. This was an expected result because A356 alloy remained in its liquid state for at least

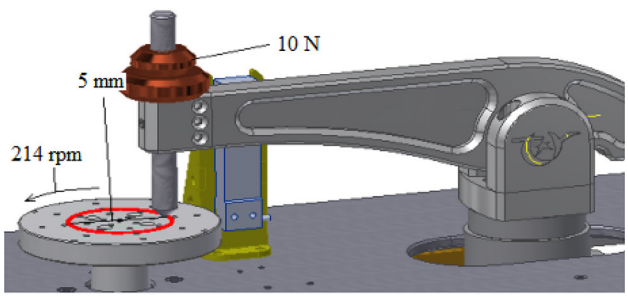


***Figure 4. Illustration of ball-on-disc test apparatus.***

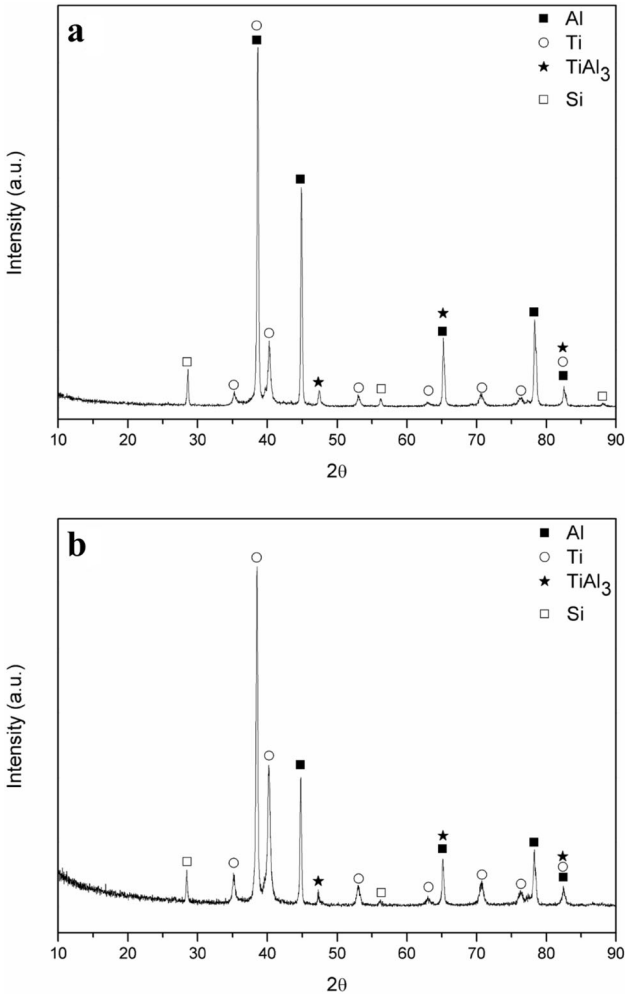


***Figure 5. X-ray diffractograms of Ti-reinforced A356 matrix composites produced by: (a) melt infiltration casting and (b) squeeze infiltration.***

1 h in SI, whereas it solidified in approximately 20 min in MIC. The presence of a slight deformation texture is observed in Figure 6b. The cover die movement downwards during melting of A356 alloy caused this texture. It can be said that production of bimetal composites was successfully accomplished with strong interfacial bonding by both MIC and SI procedures.

SEM images of Ti-reinforced A356 matrix composites are given in Figure 7. This time, dark regions indicate A356 alloy while light regions point out Ti, contrary to micrographs in Figure 6. All formed phases were demonstrated in SEM micrographs. No infiltration problem occurred at any production method, although the volume fraction of A356 alloy was quite low. Thick continuous $TiAl_3$ layers and thin α-Ti regions are shown in Figure 7b. The ordinary amount of α-Ti contained in the composite can be seen in Figure 7a. It was understood that $TiAl_3$ phase grows into α-Ti as A356 melt contacts with solid Ti.

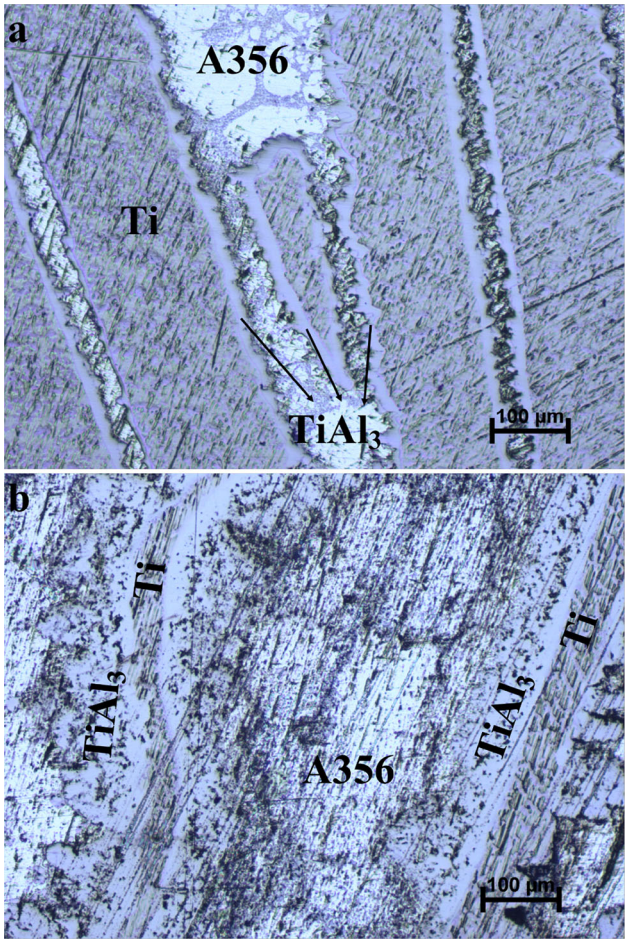


***Figure 6. Micrographs of Ti-reinforced A356 matrix composites produced by: (a) melt infiltration casting and (b) squeeze infiltration.***

At the initial stage of manufacturing, without Ti–Al interaction, the ratio of Ti/Al was arranged at 3:1 by volume for both MIC and SI. To determine the volume fraction of the final products, image analyser software was used and the results are reported in Table 3 as an average of 10 measurements. Most of the structure contains α-Ti phase in MIC, while it contains $TiAl_3$ in SI. It can be concluded that most of the reinforcement phase in SI technique was transformed to $TiAl_3$ structure by courtesy of long interaction time between liquid Al and solid Ti.

The thickness variation of $TiAl_3$ layers at the interfaces is given in Figure 8 for both production methods. Huge differences in $TiAl_3$ thicknesses between MIC and SI are crystal clear. The thickness of $TiAl_3$ in SI was found 7 times higher than that in MIC via image analyser software. Several reasons can be counted for this dramatic increase. Longer interaction time between Al and Ti in SI technique is the most important reason. The production temperature was slightly decreased with time in MIC, while it remained constant at 730 °C for 1 h in SI.

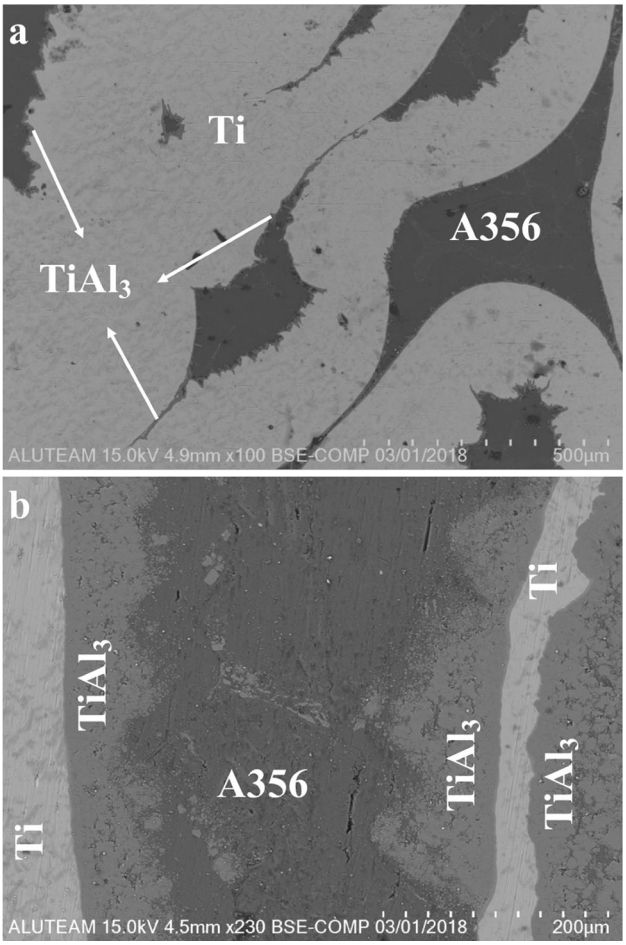


***Figure 7. SEM images of Ti-reinforced A356 matrix composites produced by: (a) melt infiltration casting and (b) squeeze infiltration.***

***Table 3. Volume Fractions of Formed Phases in Ti-Reinforced A356 Matrix Composites Produced by Melt Infiltration Casting and Squeeze Infiltration***

| Formed phases | Volume fraction (%) | |
|---|---|---|
| | Melt infiltration casting | Squeeze infiltration |
| A356 | 24.21 | 23.05 |
| Ti | 73.77 | 36.39 |
| $TiAl_3$ | 2.02 | 40.56 |

The second reason is decreased diffusion path length of A356 alloy. In MIC technique, Al has to cover a longer way to fill the voids of the preform. On the other hand, in SI method, Al has already existed in the preform and is a part of it. Thus, the diffusion of Al matrix into Ti reinforcement occurs much easier in SI system.

Nanoindentation measurements were taken to determine individual hardnesses of formed phases in bimetal

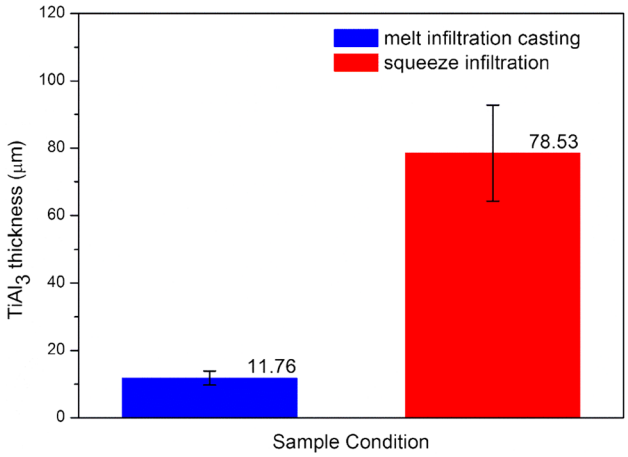


***Figure 8. $TiAl_3$ thickness values of Ti-reinforced A356 matrix composites produced by melt infiltration casting and squeeze infiltration.***

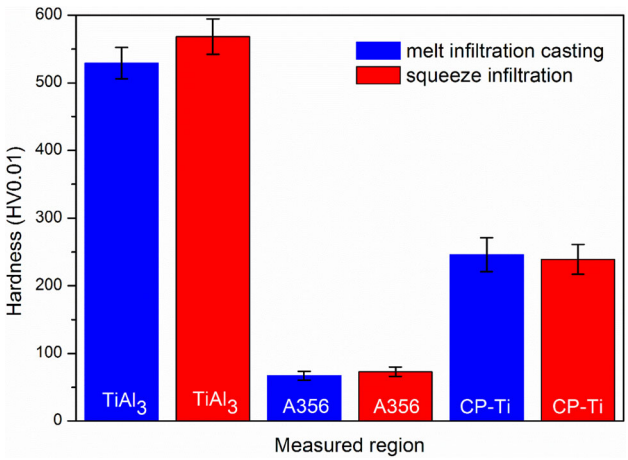


***Figure 9. Hardness of $TiAl_3$, A356 and Ti phases of Ti-reinforced A356 matrix composites produced by melt infiltration casting and squeeze infiltration.***

composite structure. Figure 9 demonstrates the hardness of $TiAl_3$, A356 and Ti phases of composite samples for both MIC and SI. The hardnesses of matrix and reinforcement sides were not significantly affected by the production method. However, $TiAl_3$ hardness was found to be a little bit higher in SI than that in MIC. The possible reason for increase in interfacial hardness of composites produced by SI method is the higher amount of diffused Si atoms in $TiAl_3$ lattice. The lattice parameter of Si is greater than that of both Al and Ti. When diffused Al and Ti atoms meet with each other, they form $TiAl_3$ structure. However, diffused Si atoms are the substitute for Ti and Al in the lattice of $TiAl_3$. Because of the larger size of Si atoms, coherent $TiAl_3$ lattice was distorted. It is well-known fact that larger mismatch causes larger induced stress. Since internal stress in composite sample produced by SI was higher due to higher amount of Si solutes, $TiAl_3$ hardness was measured higher in this method.

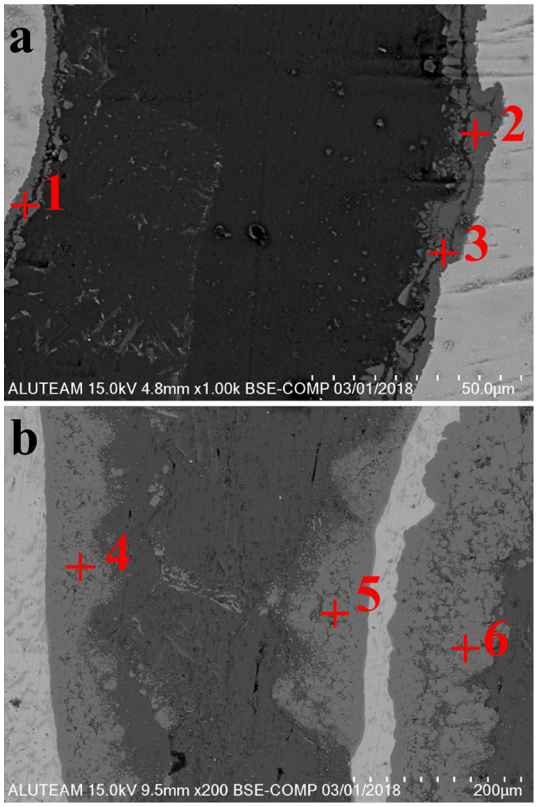


***Figure 10. EDS spots of Ti-reinforced A356 matrix composites produced by: (a) melt infiltration casting and (b) squeeze infiltration.***

SEM images consisting of EDS spots are given in Figure 10, and the related EDS results are listed in Table 4. According to the EDS results, the amount of Si was higher at the interface layer of the specimen produced by SI. This can be counted as evidence for the mentioned relationship between diffused Si atoms and the hardness of $TiAl_3$ layer.

Another remarkable point is that all constituents of composite structure were found at approximately same amounts at different spots of $TiAl_3$ phase. It can be said that the formed layer at the interface was homogeneously distributed.

Coefficient of friction (COF) values were recorded by tribometer during sliding. The average COF values of three wear tests for each specimen are given in Figure 11. According to given results, the lowest COF was recorded at composite sample produced by SI. It is a well-known fact

***Table 4. EDS Analysis Results in Figure 10 (wt%)***

| Area | Al | Si | Ti | Area | Al | Si | Ti |
|---|---|---|---|---|---|---|---|
| 1 | 58.05 | 7.77 | 34.18 | 4 | 58.65 | 9.05 | 32.3 |
| 2 | 57.46 | 8.11 | 34.43 | 5 | 58.56 | 9.28 | 32.16 |
| 3 | 59.22 | 8.02 | 33.76 | 6 | 57.78 | 9.7 | 32.52 |

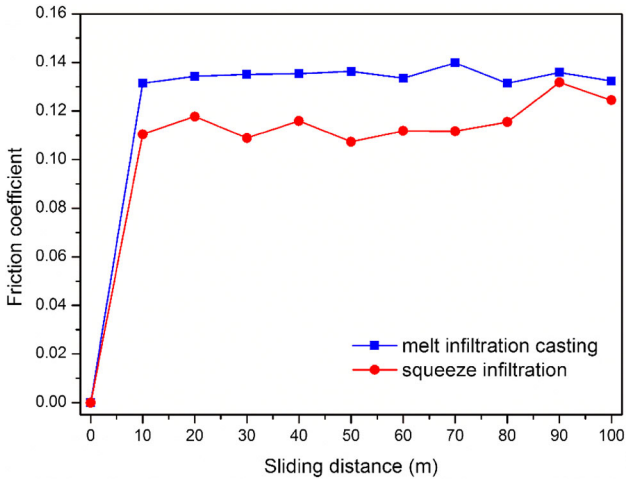


***Figure 11. Sliding distance-dependent friction coefficient values of Ti-reinforced A356 matrix composites produced by melt infiltration casting and squeeze infiltration.***

that low COF represents high wear resistance. Considering direct relationship between hardness and wear resistance,[27,28] lower COF in SI method is an expected result. However, it should be noted that the brittleness of the hard $TiAl_3$ phase may cause delamination at the interfaces and decrease in wear resistance. Tang et al.'s work[29] is a good example of the troubles of the hard sample against wear.

Sliding distance did not significantly affect the COF values. It can be said that samples reserved their steady-state condition during the entire test.

Figure 12 shows wear rates of bimetal composites produced by MIC and SI methods. Although the volume fraction of $TiAl_3$, which is a hard and brittle phase, is quite high in SI method, the wear rate of the sample produced by SI was found lower than that of the sample produced by

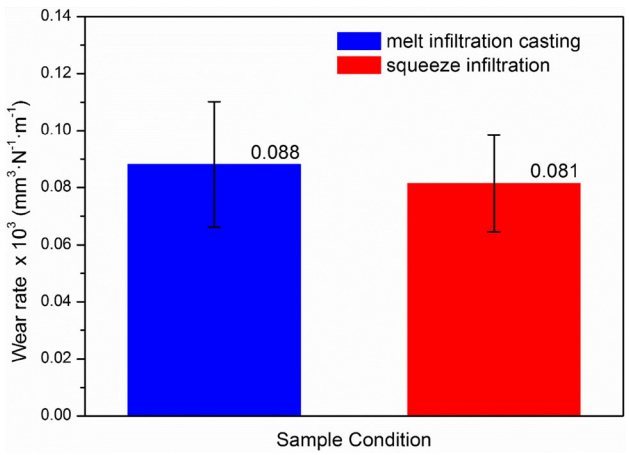


***Figure 12. Wear rate values of Ti-reinforced A356 matrix composites produced by melt infiltration casting and squeeze infiltration.***

MIC. Baron et al.[30] demonstrated the wear failure of intermetallic compound (IMC) with excessively high volume fraction, compared with optimum volume fraction. It can be inferred from Baron et al.'s work that there should be an upper limit for the volume fraction of reaction phase to enhance the tribomechanical properties of composites. The possible explanation of increase in wear resistance of sample produced by SI in spite of its high volume fraction of $TiAl_3$ is strong bonding at the interface owing to wettability of Ti, unlike conventional ceramic reinforcements. According to Delannay et al.,[31] good wetting allows load transfer from matrix to reinforcement without failure. Under favour of the good mechanical and metallurgical bonding, both samples did not suffer from the brittleness of $TiAl_3$ phase during sliding.

Worn surface SEM images of Ti-reinforced A356 matrix bimetal composites produced by MIC and SI are given in Figure 13. Predominant wear mechanism was adhesion in Al side, whereas it was abrasion in Ti side. It can be seen in Figure 13 (a) that adhesive tribolayer accumulated in Al region. Tribolayer formation can occur by plastic deformation, mechanical mixing, material transfer or debris formation.[32] With careful attention, some delaminated areas in the tribolayer can be noticed. Delamination wear indicates that the material is exposed to plastic deformation. Under these conditions, it can be inferred that plastic deformation is the main reason for tribolayer formation in A356 side.

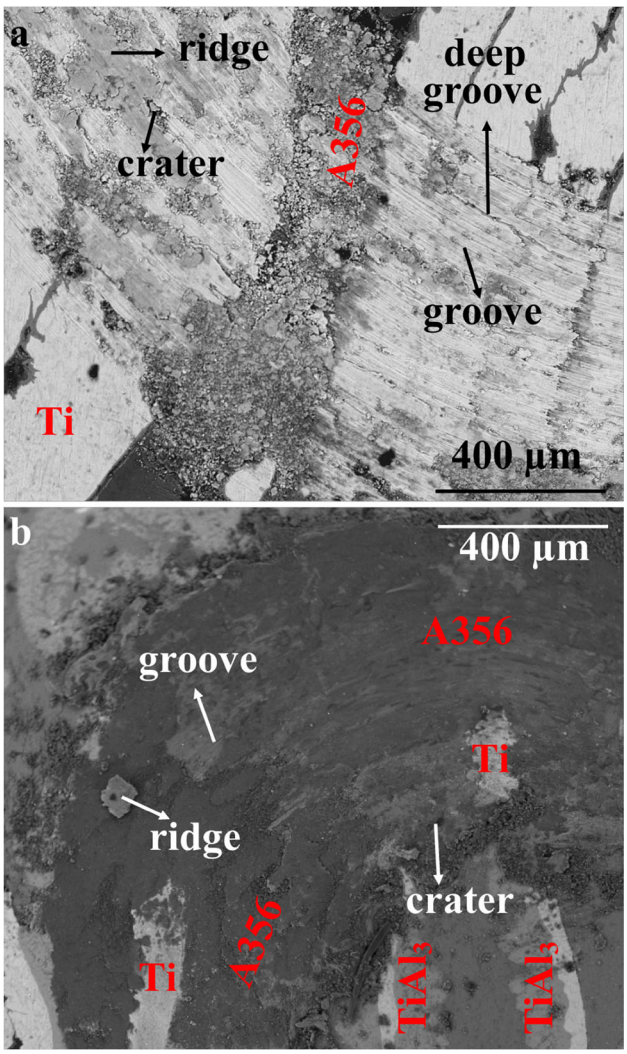


***Figure 13. Worn surface SEM images of Ti-reinforced A356 matrix composites produced by melt infiltration casting and squeeze infiltration.***

The sample produced by MIC was exposed to more plastic deformation than the sample produced by SI. Since the component exposed to the most plastic deformation in the composite structure is Al alloy, the specimen produced by MIC suffered from more deformation. Table 3 demonstrates that the amount of A356 alloy was higher in MIC than that in SI. Besides, delamination explains high wear debris density in Al side of sample produced by MIC, because according to Suh,[33] delamination causes wear debris formation.

$TiAl_3$ layers adjacent to the wear traces were not damaged after wear test for both specimens. It is well-known fact that most suitable regions for the nucleation and the propagation of the cracks are interfaces due to their high stress concentration.[34] However, $TiAl_3$ fragmentation did not occur in any of the bimetal composites. The deterioration of the interface would multiply wear rate if the bonding was weak. Fortunately, whether thin or thick, $TiAl_3$ phase was strongly bonded to matrix and reinforcement phases and provided better wear resistance. It can be said that increased thickness, hardness and volume fraction of $TiAl_3$ provided increase in wear resistance.

Ridges and craters as evidence of adhesive wear and grooves can be seen in Figure 13a, b explicitly. Detached particles from composites were plastered to $Al_2O_3$ ball during sliding. If plastered particles remained in counter material, there should be a crater in composite structure. If they participated in the composite again, there should be a ridge. Apparently, detached particles of bimetal composites exhibited both behaviours.

Some deep grooves can be noticed in Figure 13a. Deeper grooves in sample produced by MIC than sample produced by SI proved that abrasive wear rate was higher in MIC under the same test conditions. These worn surface images were totally in agreement with the COF and wear rate values shown in Figs. 11 and 12, respectively.

## Conclusion

Ti-reinforced A356 matrix composites were successfully produced by MIC and SI techniques with good interfacial contact between Al and Ti phases. No defects were resulted

from vacuum assistance in MIC and cover die pressure in SI. Low cost and environmentally friendly production became possible under favour of waste utilization.

Al, Ti, Si and $TiAl_3$ phases were obtained by XRD analysis. $TiAl_3$ is the only formed phase at the interfaces among all titanium aluminide compounds. Single layer helps avoid detrimental effects of complex formations. The volume fraction, thickness and hardness of $TiAl_3$ layer were obtained higher in SI than those in MIC. Longer interaction time between liquid Al and solid Ti allowed the growth of $TiAl_3$ phase. Increased amount of Si solutes in $TiAl_3$ lattice was the main reason for higher $TiAl_3$ hardness in SI method.

Worn surface examinations revealed that predominant wear mechanisms were adhesion and abrasion for Al and Ti sides, respectively. Sample produced by MIC was exposed to more plastic deformation and abrasive wear than sample produced by SI. In spite of the higher initial investment cost, SI technique seems more advantageous than MIC, considering the tribological features of bimetal composites and applicability of the process in the industry.

## Acknowledgement

This research was supported by Yildiz Technical University Scientific Research Projects Coordination Department with the project number of FDK-2017-3241.

## REFERENCES

1. S.J.S. Chelladurai, R. Arthanari, R. Selvarajan, R. Kanagaraj, P. Angappan, Trans. Indian Inst. Met. (2018). https://doi.org/10.1007/s12666-018-1353-5
2. M. Singh, R.S. Rana, R. Purohit, K. Sahu, Mater. Today Proc. **2**, 3697 (2015)
3. M. Tan, Q. Xin, Z. Li, B.Y. Zong, J. Mater. Sci. **6**, 2045 (2001)
4. D.L. Zalensas, *Aluminum Casting Technology*, 2nd edn. (American Foundry Society, Schaumburg, 1997)
5. S. Bao, K. Tang, A. Kvithyld, T. Engh, M. Tangstad, Trans. Nonferrous Met. Soc. China (English Ed.) **22**, 1930 (2012)
6. A. Hosseini Monazzah, H. Pouraliakbar, R. Bagheri, S.M. Seyed Reihani, Compos. Part B Eng. **125**, 49 (2017)
7. J. Park, J. Lee, I. Jo, S. Cho, S.K. Lee, S.B. Lee, H.J. Ryu, S.H. Hong, Surf. Coat. Technol. **307**, 399 (2016)
8. X.Y. Nie, J.C. Liu, H.X. Li, Q. Du, J.S. Zhang, L.Z. Zhuang, Mater. Des. **63**, 142 (2014)
9. S.V. Prasad, R. Asthana, Tribol. Lett. **17**, 445 (2004)
10. R. Gecu, A. Karaaslan, Tribol. Lett. **65**, 164 (2017)
11. S.K. Thakur, M. Gupta, Compos. Part A Appl. Sci. Manuf. **38**, 1010 (2007)
12. Y. Milman, D. Miracle, S. Chugunova, Intermetallics **9**, 839 (2001)
13. A.R. Rastkar, P. Parseh, N. Darvishnia, S.M.M. Hadavi, Appl. Surf. Sci. **276**, 112 (2013)
14. S. Djanarthany, J.C. Viala, J. Bouix, Mater. Chem. Phys. **72**, 301 (2001)
15. B. Guo, S. Ni, R. Shen, M. Song, Mater. Sci. Eng. A **639**, 269 (2015)
16. G. Wu, Y. Liu, Z. Xiu, L. Jiang, W. Yang, Rare Met. **29**, 98 (2010)
17. H. Kwon, J. Mondal, K. AloGab, V. Sammelselg, M. Takamichi, A. Kawaski, M. Leparoux, J. Alloys Compd. **698**, 807 (2017)
18. S.J.S. Chelladurai, R. Arthanari, K. Krishnamoorthy, K.S. Selvaraj, P. Govindan, Trans. Indian Inst. Met. **71**, 1 (2018)
19. B.C. Kandpal, J. Kumar, H. Singh, Mater. Today Proc. **4**, 2783 (2017)
20. G.M. Karthik, G.D.J. Ram, R.S. Kottada, Mater. Sci. Eng. A **653**, 71 (2016)
21. S.F. Hassan, M. Gupta, Mater. Res. Bull. **37**, 377 (2002)
22. J.E. Allison, G.S. Cole, JOM **45**, 19 (1993)
23. A. Loukus, J. Loukus, Int. J. Met. **5**, 57 (2011)
24. G.A. Gegel, D.J. Weiss, Int. J. Met. **1**, 57 (2007)
25. H. Nakae, Y. Hiramoto, Int. J. Met. **5**, 23 (2011)
26. J.C. Schuster, M. Palm, J. Phase Equilib. Diffus. **27**, 255 (2006)
27. J.D. Lemm, A.R. Warmuth, S.R. Pearson, P.H. Shipway, Tribol. Int. **81**, 258 (2014)
28. J. Li, Y. Lu, H. Zhang, L. Xin, Tribol. Int. **81**, 215 (2015)
29. L. Tang, C. Gao, J. Huang, H. Zhang, W. Chang, Tribol. Int. **66**, 165 (2013)
30. R. Baron, J. Wert, D. Gerard, F. Wawner, J. Mater. Sci. **32**, 6435 (1997)
31. F. Delannay, L. Froyen, A. Deruyttere, J. Mater. Sci. **22**, 1 (1987)
32. F.H. Stott, Tribol. Int. **35**, 489 (2002)
33. N.P. Suh, Wear **25**, 111 (1973)
34. S. Sawla, S. Das, Wear **257**, 555 (2004)